



# pH EFFECT ON STRUCTURAL, MORPHOLOGICAL AND OPTICAL PROPERTIES OF ZnO THIN FILMS PRODUCED BY CHEMICAL BATH DEPOSITION METHOD

M. Fatih Gözükızıl<sup>[a]\*</sup>

**Keywords:** Chemical bath deposition, ZnO, thin films, pH effect.

Zinc oxide (ZnO) thin films are widely used in the production of high value-added technological products such as photovoltaic cells, sensors, flexible and wearable electronic materials, as they are abundant in nature, easy to process, low cost and can be produced with different methods. The Chemical Bath Deposition method is preferred in the production of metal oxide thin films by changing the parameters such as pH, temperature and concentration by immersing the various substrates into the prepared solution without the need for a vacuum environment. In this study, ZnO thin films were grown on glass substrates by chemical bath deposition method. The effects of pH on the structural, morphological and optical properties of the obtained films were investigated using X-ray diffraction (XRD) method, Field Emission Scanning Electron Microscopy (FESEM) and UV-Vis Spectrophotometry respectively. It was observed that the optimum film formation took place in the Z3 series at pH 10.

\* Corresponding Authors

E-Mail: faith.gozukizil@bilecik.edu.tr

[a] Bilecik Seyh Edebali University Söğüt Vocational School, 11230, Bilecik, Turkey

## INTRODUCTION

With the development of increasing technology and application techniques, thin films can be deposited on different morphologicals by using many metal oxides such as cadmium oxide,<sup>1</sup> copper oxide,<sup>2</sup> zinc oxide,<sup>3</sup> magnesium oxide,<sup>4</sup> titanium dioxide,<sup>5,6</sup> and vanadium oxide.<sup>7</sup> Metal oxide thin films can be obtained as a result of the combination of many techniques such as sol-gel spin coating,<sup>8</sup> pulse laser deposition,<sup>9,10</sup> chemical bath deposition (CBD),<sup>11,12</sup> and chemical spray pyrolysis.<sup>13</sup> Due to their electrical conductivity,<sup>14</sup> optical transmittance<sup>15,16</sup> and special band gaps, metal oxide thin films can be produced by using different techniques according to their usage areas and desired features.<sup>17</sup> ZnO thin films do not contain toxic chemicals, are suitable for developing alternative structures, easy-to-find and low cost. It is used as a value-added product in many different areas up to water treatment.<sup>18-24</sup> Metal oxide thin film deposition by chemical bath deposition method is more preferred than other techniques due to its advantages such as low cost, simple application<sup>25</sup> and easy change of parameters as temperature<sup>26</sup> and pH.<sup>27</sup> The system does not require quick and additional annealing. In this study, ZnO thin films were produced by preparing bath solutions at different pH values with the CBD method, and the effects of the solution pH value on the structural, morphological and optical properties of thin films were investigated.

## EXPERIMENTAL

CBD method is the method of obtaining a film on suitable substrate at suitable temperature by using the chemicals prepared with an aqueous solution with suitable

stoichiometry. In this method, the substrate is immersed in the prepared chemical bath and there is no need for vacuum environment to produce the film and the pH of the solution plays an important role and the pH and temperature of the solution must be kept the same during film formation. In order to produce ZnO films by CBD method, a 0.25 M zinc nitrate hexahydrate  $Zn(NO_3)_2 \cdot 6H_2O$  (Sigma Aldrich) solution was prepared. Then 28 % aqueous ammonia ( $NH_4OH$ ) (Merck) was added to the solution to adjust the pH of the solution. To examine the effect of pH value on thin films, 4 different pH values were chosen and solutions were prepared. The naming of the selected pH values and series are given in Table 1.

**Table 1.** Series naming by pH values.

pH	Series Name
9	Z1
9.5	Z2
10	Z3
10.5	Z4

After the solutions were prepared, the pre-cleaned glass substrate was immersed in the bath and the solution was started to be heated while mixing the solution with the help of a heated and temperature controlled magnetic mixer. The immersed films were kept in the bath for 30 min at 85 °C bath temperature. The coated films were removed from the bath. The removed films were washed with distilled water and dried outdoors. The X-ray diffraction (XRD) method was used for the structural characterization of the films obtained. PANALYTICAL Empyrean X-Ray Diffraction (XRD) device was used to examine the structural properties of the films obtained. 45 kV voltage and 40 mA current are applied as operating conditions of the device. The scanning speed was selected at 2 degrees / minute, the wavelength of 1.5406 Å was used with  $CuK_{\alpha}$  beam and samples were examined at  $30^{\circ} \leq 2\theta \leq 60^{\circ}$  limit values. Morphological properties were investigated using Field Emission Scanning Electron Microscopy (FESEM) and optical properties using UV-Vis Spectrophotometry.

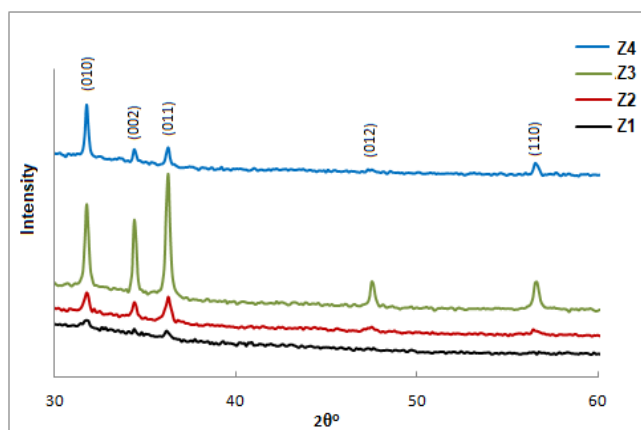


Figure 1. XRD spectra of ZnO thin films.

## RESULTS AND DISCUSSION

As seen in Figure 1, all series are polycrystalline and show peaks of hexagonal ZnO structure. Peak intensities of films prepared as pH 10 in Z3 series are higher than peak intensities of other series. In the Z1 series, the crystallinity of the films prepared at pH 9 is quite low. As can be seen from the spectrum, the peaks of the (010), (002) and (011) planes belonging to the hexagonal ZnO structure started to appear in the Z1 series with very low intensities. In the Z2 series, when the pH value was brought to 9.5, the intensities of the peaks of the same planes also increased. In addition, the peaks of the (012) and (110) planes of the hexagonal ZnO structure were observed at low intensities. In the Z3 series, all of the (010), (002), (011), (012) and (110) peaks of the hexagonal ZnO structure were formed violently and sharply in the films prepared at pH 10.

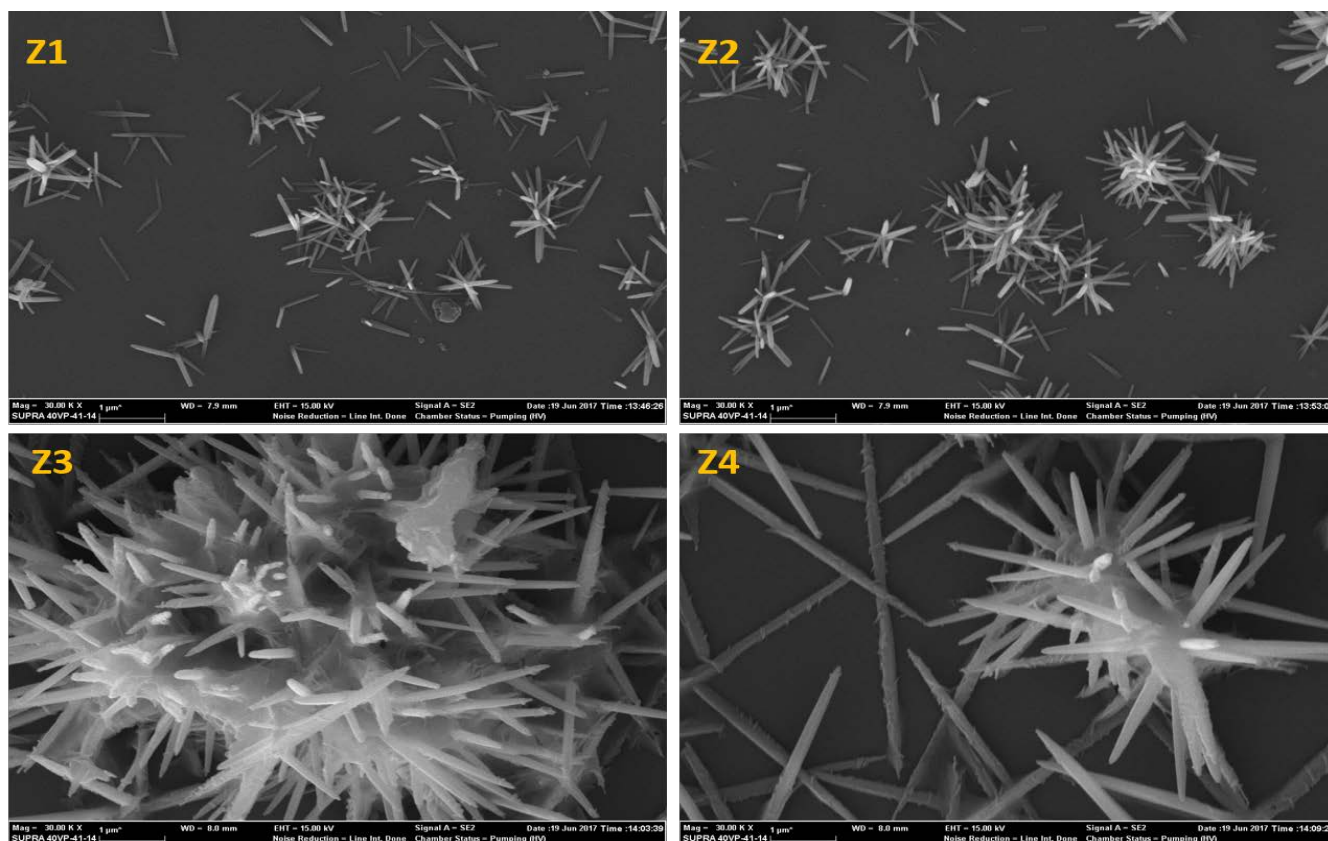


Figure 2. FESEM images of ZnO thin films.

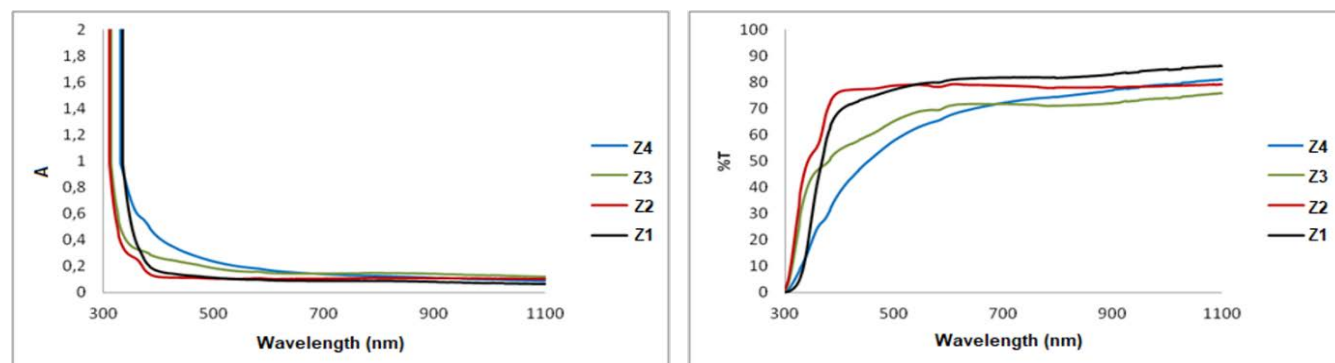


Figure 3. Absorbance and optical transmittance spectra of ZnO thin films.

As can be seen from the spectrum, the Z3 series is the series with the most severe peaks. Z3 series has preferential orientation in the direction of (011) peak formed at  $2\theta \approx 36.24^\circ$ . In the Z4 series, when the pH value was brought to 10.5, a reduction of the intensity of the peaks of the hexagonal ZnO structure was observed.

In Table 2, the full width half maximum (FWHM) and average grain size (D) values of thin films are given. With the information obtained from XRD spectra; The wavelength of the x-ray used is  $\lambda$ , the diffraction angle is  $\theta$  and the half peak width in radians is  $\beta$ , and the average grain sizes of the films are calculated using the Scherrer formula.<sup>28</sup>

$$D = 0.9\lambda/\beta\cos\theta \quad (1)$$

In the Z3 series, it is seen that the grain size value is greater than 53 nm. Crystallization improves as grain sizes increase. In addition, as the full width half maximum (FWHM) decreases, crystallization improves. Considering all these data, it is understood that the best crystallization is seen in the films of Z3 series.

**Table 2.** Grain size values of thin films.

Serial name	FWHM	D, nm
Z1	0,3133	25
Z2	0,2199	39
Z3	0,1789	53
Z4	0,1966	44

ZEISS Supra 40VP Field Emission Scanning Electron Microscope (FESEM) was used to examine the morphological properties of ZnO thin films produced at different pH values. While examining the morphological properties of the device, the secondary electron (SE) detector was used and images at 30 kx magnification were obtained.

When the FESEM images given in Figure 2 are examined, it is seen that the films consist of continuous and independent nano sticks. It is also seen that these nano sticks combine to form a flower-like structure. Average grain size values calculated from FESEM images are in the range of 40-50 nm. In the Z1 and Z2 series, it is shown in the FESEM image that there are voids on the morphological and the structure is not completely formed. This data confirms the XRD results.

UV-Vis Spectroscopy measurements were taken in the range of 300-1100 nm in PERKIN ELMER LAMBDA 25 to examine the optical properties of the films obtained.

In Figure 3, absorption spectra and optical transmittance spectra of ZnO thin films at room temperature are given comparatively. The band gap values of the thin film was calculated by using Tauc method.<sup>29</sup> The band gap value calculated for each series is given in Table 3.

**Table 3.** Band gap values of ZnO thin films.

Series name	Bandgap values, eV
Z1	3.21
Z2	3.26
Z3	3.35
Z4	3.27

The band gap values of ZnO thin films are reported in the literature as about 3.3 eV.<sup>30-32</sup> When Table 3 is examined, the series closest to this value is the Z3 series. In addition, as seen in Figure 3, with the increase in pH value, a decrease in optical transmittance spectra is observed in the visible region (400 - 700 nm).

## CONCLUSION

In this study, ZnO thin films were produced on glass substrates by CBD method. Solutions were prepared by selecting 4 different pH values between pH 9.5-10.5 values, series were named and the effect of pH on thin films was examined. When the structural properties of the films obtained were examined by the X-ray diffraction (XRD) method, it was observed that the 4 different series contain peaks of the polycrystalline structure and hexagonal ZnO structure, and the peak intensities of the films prepared in the Z3 series as pH 10 are higher than the peak intensities of the other series. When the full width half maximum (FWHM) and average grain size (D) values were calculated, it was observed that the grain size value in the Z3 series was higher than the others with 53 nm and crystallization improved as the grain sizes increased. Therefore, it was understood that the best crystallization was seen in the films of Z3 series. When the morphological properties of ZnO thin films produced at different pH values were examined by Field Emission Scanning Electron Microscope (FESEM), it was observed that they consist of independent nano sticks, combine to form a flower-like structure, and average grain size values are in the range of 40-50 nm. When the optical properties of the films were examined by UV-Vis Spectroscopy measurements. The band gap values of the Z3 series of thin films was calculated as 3.35 eV with the Tauc method. It is observed that optimum film formation occurs in the Z3 series at pH 10, where crystallization is the best compared to other series.

## REFERENCES

- Mane, R. S., Pathan, H. M., Lokhande, C. D., Han, S. H., An effective use of nanocrystalline CdO thin films in dye-sensitized solar cells, *Sol. Energy*, **2006**, *80*(2), 185–190. <https://doi.org/10.1016/j.solener.2005.08.013>
- Sahu, K., Choudhary, S., Khan, S. A., Pandey, A., Mohapatra, S., Thermal evolution of morphological, structural, optical and photocatalytic properties of CuO thin films, *Nano-Struct. Nano-Objects*, **2019**, *17*, 92–102. <https://doi.org/10.1016/j.nanoso.2018.12.005>
- Temel, S., Influence of deposition temperature on structural, morphological and optical properties of ZnS thin films, *Can. J. Phys.*, **2018**, *96*, 826–830. <https://doi.org/10.1139/cjp-2017-0730>

- <sup>4</sup>Tigunta, S., Sando, D., Chanlek, N., Supadee, L., Pojprapai, S., Effect of gas atmospheres on degradation of MgO thin film magnetic tunneling junctions by deionized water, *Thin Solid Films*, **2020**, 709, 138185. <https://doi.org/10.1016/j.tsf.2020.138185>
- <sup>5</sup>Pawlak, J. J., Al-Ani, S. K. J., Inverse logarithmic derivative method for determining the energy gap and the type of electron transitions as an alternative to the Tauc method, *Opt. Mater.*, **2019**, 88, 667–673. <https://doi.org/10.1016/j.optmat.2018.12.041>
- <sup>6</sup>Sun, Z., Pichugin, V. F., Evdokimov, K. E., Konishchev, M. E., Syrtanov, M. S., Kudiyarov, V. N., Tverdokhlebov, S. I., Z., Effect of nitrogen-doping and post annealing on wettability and band gap energy of TiO<sub>2</sub> thin film, *Appl. Sur. Sci.*, **2020**, 500, 144048. <https://doi.org/10.1016/j.apsusc.2019.144048>
- <sup>7</sup>Türhan, I., Tepehan, G. G., Properties of tantalum mixed vanadium oxide thin film, *ITU Dergisi/C*, **2009**, 7(1), 27-37.
- <sup>8</sup>Temel, S., Nebi, M., Peker, D., Sol-Gel Döndürerek Kaplama Tekniği ile Saydam İletken ZnO İnce Filmlerin Üretilmesi ve Karakterizasyonu, *GU J Sci, Part C*, **2017**, 5(3): 51-59.
- <sup>9</sup>De León, J. G., Pérez-Centeno, A., Gómez-Rosas, G., Mariscal, A., Serna, R., Santana-Aranda, M. A., & Quiñones-Galván, J. G., Influence of the Zn plasma kinetics on the structural and optical properties of ZnO thin films grown by PLD, *SN Appl. Sci.*, **2019**, 1(5), 475. <https://doi.org/10.1007/s42452-019-0497-1>
- <sup>10</sup>Kang, H. S., Ahn, B. D., Kim, J. H., Kim, G. H., Lim, S. H., Chang, H. W., & Lee, S. Y. Structural, electrical, and optical properties of p-type ZnO thin films with Ag dopant, *Appl. Phy. Lett.*, **2006**, 88(20), 202108. <https://doi.org/10.1063/1.2203952>
- <sup>11</sup>Temel, S., Bath Temperature Effect on c-axis Preferred Orientations and Band Gap of Semiconductor ZnO Thin Films, *BSEU J. Sci. Araştırma Makalesi-Research Article*, **2019**, 6(1), 24–28. <https://doi.org/10.35193/bseufbd.550769>
- <sup>12</sup>Temel, S., Gökmen, F., Yaman, E., An energy efficient way to produce zinc-based semiconductor thin films via chemical bath deposition technique, *J. Sustain. Dev. Energy Water Environ.*, **2019**, 7(2), 253–260. <https://doi.org/10.13044/j.sdewes.d6.0239>
- <sup>13</sup>Hunge, Y. M., Yadav, A. A., Kulkarni, S. B., Mathe, V. L., A multifunctional ZnO thin film based device for photoelectrocatalytic degradation of terephthalic acid and CO<sub>2</sub> gas sensing applications, *Sensor. Actuators, B-Chem.*, **2018**, 274, 1-9. <https://doi.org/10.1016/j.snb.2018.07.117>
- <sup>14</sup>Abliz, A., Xu, L., Wan, D., Duan, H., Wang, J., Wang, C., Liu, C. Effects of yttrium doping on the electrical performances and stability of ZnO thin-film transistors, *Appl. Sur. Sci.*, **2019**, 475, 565–570. <https://doi.org/10.1016/j.apsusc.2018.12.236>
- <sup>15</sup>Sarma, B., Barman, D., Sarma, B. K., AZO (Al:ZnO) thin films with high figure of merit as stable indium free transparent conducting oxide, *Appl. Sur. Sci.*, **2019**, 479, 786–795. <https://doi.org/10.1016/j.apsusc.2019.02.146>
- <sup>16</sup>Benramache, S., Fabrication and Characterisation of ZnO Thin Film by Sol–Gel Technique, *Ann. West Univ. Timisoara-Phy.*, **2020**, 61(1), 64–70. <https://doi.org/10.2478/awutp-2019-0006>
- <sup>17</sup>Chandrasekar, L. B., Nagarajan, S., Karunakaran, M., Thangadurai, T. D., Structural, Optical and Electrical Properties of Undoped and Doped ZnO Thin Films, *2D Materials*, **2019**, IntechOpen <https://doi.org/10.5772/intechopen.88905>
- <sup>18</sup>Zaka, H., Parditka, B., Erdélyi, Z., Atyia, H. E., Sharma, P., Fouad, S. S., “Investigation of dispersion parameters, dielectric properties and opto–electrical parameters of ZnO thin film grown by ALD, *Optik*, **2020**, 203, 163933. <https://doi.org/10.1016/j.ijleo.2019.163933>
- <sup>19</sup>Wang, M., Li, X., Xiong, X., Song, J., Gu, C., Zhan, D., Wu, Y. High-Performance Flexible ZnO Thin-Film Transistors by Atomic Layer Deposition, *IEEE Electron Device Lett.*, **2019**, 40(3), 419–422. <https://doi.org/10.1109/LED.2019.2895864>
- <sup>20</sup>Ghosh, A., Zhang, C., Zhang, H., Shi, S., CO<sub>2</sub> Sensing Behavior of Calcium-Doped ZnO Thin Film: A Study to Address the Cross-Sensitivity of CO<sub>2</sub> in H<sub>2</sub> and CO Environment, *Langmuir*, **2019**, 35(32), 10267–10275. <https://doi.org/10.1021/acs.langmuir.9b00724>
- <sup>21</sup>Parellada-Monreal, L., Castro-Hurtado, I., Martínez-Calderón, M., Presmanes, L., Mandayo, G. G. Laser-induced periodic surface structures on ZnO thin film for high response NO<sub>2</sub> detection, *Appl. Sur. Sci.*, **2019**, 476, 569–575. <https://doi.org/10.1016/j.apsusc.2019.01.115>
- <sup>22</sup>Ghosh, A., Zhang, C., Shi, S., Zhang, H., High temperature CO<sub>2</sub> sensing and its cross-sensitivity towards H<sub>2</sub> and CO gas using calcium doped ZnO thin film coated langasite SAW sensor, *Sensor. Actuators, B-Chem.*, **2019**, 301, 126958. <https://doi.org/10.1016/j.snb.2019.126958>
- <sup>23</sup>Tao, K., Yi, H., Tang, L., Wu, J., Wang, P., Wang, N., Chang, H. Piezoelectric ZnO thin films for 2DOF MEMS vibrational energy harvesting, *Surf. Coat. Technol.*, **2019**, 359, 289-295. <https://doi.org/10.1016/j.surfcoat.2018.11.102>
- <sup>24</sup>Tekin, D., Tekin, T., Kiziltas, H., Photocatalytic degradation kinetics of Orange G dye over ZnO and Ag/ZnO thin film catalysts, *Sci. Rep.*, **2019**, 9(1), 1–7. <https://doi.org/10.1038/s41598-019-54142-w>
- <sup>25</sup>Thamaraiselvan, C., Carmiel, Y., Eliad, G., Sukenik, C. N., Semiat, R., Dosoretz, C. G., Modification of a polypropylene feed spacer with metal oxide-thin film by chemical bath deposition for biofouling control in membrane filtration, *J. Membrane Sci.*, **2019**, 573, 511–519. <https://doi.org/10.1016/j.memsci.2018.12.033>
- <sup>26</sup>Waldiya, M., Narasimman, R., Bhagat, D., Vankhade, D., Mukhopadhyay, I., Nanoparticulate CdS 2D array by chemical bath deposition: Characterization and optoelectronic study, *Mater. Chem. Phys.*, **2019**, 226, 26–33. <https://doi.org/10.1016/j.matchemphys.2019.01.017>
- <sup>27</sup>Terasako, T., Obara, S., Sakaya, S., Tanaka, M., Fukuoka, R., Yagi, M., Yamamoto, T. Morphology-controlled growth of ZnO nanorods by chemical bath deposition and seed layer dependence on their structural and optical properties, *Thin Solid Films*, **2019**, 669, 141–150. <https://doi.org/10.1016/j.tsf.2018.10.039>
- <sup>28</sup>Cullity, B. D., Stock, S. R., *Elements of x-ray diffraction*. Prentice Hall, Dundee, Scotland, **2001**.
- <sup>29</sup>Tauc, J., *Amorphous and Liquid Semiconductors*, Springer USA, **1974**. <https://doi.org/10.1007/978-1-4615-8705-7>
- <sup>30</sup>Chaudhari, K. B., Rane, Y. N., Shende, D. A., Gosavi, N. M., Gosavi, S. R., Effect of annealing on the photocatalytic activity of chemically prepared TiO<sub>2</sub> thin films under visible light, *Optik*, **2019**, 193, 163006. <https://doi.org/10.1016/j.ijleo.2019.163006>
- <sup>31</sup>Sharmin, M., Bhuiyan, A. H., Modifications in structure, surface morphology, optical and electrical properties of ZnO thin films with low boron doping, *J. Mater. Sci.-Mater. El.*, **2019**, 30(5), 4867–4879. <https://doi.org/10.1007/s10854-019-00781-8>
- <sup>32</sup>Urper, O., Baydogan, N., Influence of structural changes on electrical properties of Al:ZnO films, *Mater. Lett.*, **2020**, 258, 126641. <https://doi.org/10.1016/j.matlet.2019.126641>

Received: 05.08.2020.

Accepted: 20.08.2020.